American Mineralogist, Volume 75, pages 755–763, 1990

Mössbauer and X-ray study of the effects of vacancy concentration in synthetic hexagonal pyrrhotites

Olof Kruse*

Department of Mineralogy and Petrology, Institute of Geology, Uppsala University, Box 555, S-751 22 Uppsala, Sweden

Abstract

Homogeneous samples of hexagonal pyrrhotite ($Fe_{1-x}S$) in the compositional range $0.004 \leq x \leq 0.143$, obtained by dry synthesis followed by quenching, were studied by X-ray diffractometry and Mössbauer spectroscopy. Spectra were recorded at ~285 K and at 77 K for two of the samples. Spectra were analyzed by a full Hamiltonian procedure. For $0.004 \leq x \leq 0.042$, a total of three sextets were assigned to (1) Fe atoms forming triangular clusters typical of the troilite structure, without any vacancies among the eight nearest neighbors, (2) cluster members with one vacancy among the eight nearest neighbors, and (3) Fe atoms not being cluster members. For $0.054 \leq x \leq 0.079$, spectra consist of several overlapping sextets. Two of these sextets correspond to Fe atoms with zero or one vacancy among the eight nearest Fe positions. For $0.106 \leq x \leq 0.143$, three sextets correspond to Fe atoms with zero, one, or two vacancies among the eight nearest Fe positions. The two-vacancy case is restricted to compositions for which monoclinic pyrrhotite is reported and may be a prerequisite for its formation. At room temperature, repulsive forces prohibit the two-vacancy case for hexagonal pyrrhotite; it may, however, occur with increased temperature. Coupled with ordering of vacancies into every other Fe layer, this could explain the transformation of normal hexagonal pyrrhotite with large x values into the $4C$-superstructure type on heating. An α transition was encountered for $x \approx 0.045$ at room temperature. A mechanism for the transition is proposed.

Introduction

Owing to their petrological importance and crystallographic, magnetic, and electric properties, phases of composition $Fe_{1-x}S$ have interested many authors. Phase relations are complicated and, despite considerable effort, not completely understood at present. A phase diagram is given in Figure 1. Hägg and Sucksdorff (1933) carried out X-ray studies of a series of phases (dry synthesis, quenched samples) where x was varied and showed the variation to be due to vacant metal positions. The superstructure found in troilite, FeS, was detected also in samples with $x \leq 0.047$ at ambient conditions, but not for larger values of x. Portions of the NiAs and troilite crystal structures are compared in Figure 2. In a similar investigation, Fleet (1968) observed abrupt cell-parameter discontinuities close to this critical composition. These discontinuities could, however, not be confirmed in a later investigation and literature review (Barker and Parks, 1986).

In addition, Mössbauer studies of synthetic samples yield contradictory results. For small values of x, only one sextet (indicating one type of Fe position) is reported up to $x = 0.065$ (Ono et al., 1962), $x = 0.077$ (Schwartz and Vaughan, 1972), and $x = 0.07$ (Gosselin et al., 1976). Goncharov et al. (1970) reported two sextets for $0.048 \leq x \leq 0.091$ and three sextets for larger values of x. Onufrienok and Zvegintsev (1982) observed line broadening for $x = 0.091$ and attributed it to three overlapping sextets. Igaki et al. (1981 and 1982) attempted to correlate the intensities of overlapping peaks in the range $0.08 \leq x \leq 0.125$ to calculated probabilities of different environments around the Fe atoms. Despite "poor resolution due to the closely spaced peak positions," the patterns were explained as resulting from nine sextets.

Ovanesyan et al. (1971) correlated Mössbauer data with different assumed Fe environments in natural pyrrhotite samples. However, the small compositional range ($0.091 \leq x \leq 0.119$) in their investigation did not allow a general analysis of the effects of vacancy concentration.

The present work is an attempt to investigate the effects of vacancies in pyrrhotite by Mössbauer spectroscopy and X-ray diffraction. Synthetic samples were used to avoid the intimate coexistence of several $Fe_{1-x}S$ phases commonly encountered in natural specimens (Putnis and McConnell, 1980). The high temperature $1C$ structure is unquenchable (Kissin and Scott, 1982). However, the metastable superstructures formed on rapid cooling have very large cell dimensions that are functions of the exact compositions. It is implied below that formation of these superstructures does not affect the short range surroundings of the Fe atoms.

* Present address: Seco Tools AB S-773 01 Fagersta, Sweden.

0003–004X/90/0708–0755$02.00

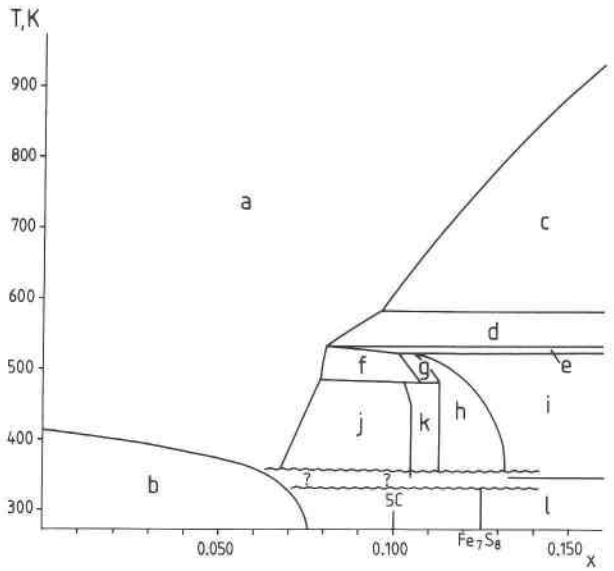

Fig. 1. Phase diagram for $Fe_{1-x}S$. Simplified largely after Kissin and Scott (1982) and Kissin (1974). Crystal systems are given as hexagonal or monoclinic as detected by diffractometry excluding low-angle superstructure reflections of low intensity. Terminology from Nakazawa and Morimoto (1971). (a) hexagonal pyrrhotite of 1*C* type, i.e., NiAs structure without superstructure; (b) hexagonal troilite (FeS with $\sqrt{3}A/2C$ superstructure, i.e., $a = \sqrt{3}A$ and $c = 2C$ where A and C are the axes of the NiAs subcell common to troilite and pyrrhotite) + hexagonal $Fe_{1-x}S$; (c) 1*C* type + pyrite (FeS_2); (d) hexagonal *MC* type (2*A*/*MC*; *M* varies continuously between 3.0 and 4.0) + pyrite; (e) hexagonal *NA* type (*NA*/3*C*; *N* varies continuously between 40 and 90) + pyrite; (f) *NA* type; (g) *NA* type + 4*C* monoclinic pyrrhotite; (h) 4*C* type monoclinic pyrrhotite; (i) 4*C* type + pyrite; (j) hexagonal *NC* type (2*A*/*NC*; *N* varies continuously between 6.0 and 3.0); (k) *NC* type + 4*C* monoclinic pyrrhotite; (l) monoclinic pyrrhotite + smythite ($Fe_{3+x}S_4$, where x varies between 0.24 and 0.30). Low-temperature relations are unclear and difficult to define owing to metastable behavior. *NC* type pyrrhotites are represented in natural assemblages by discrete phases, with *N* assuming values between 4.88 and 6.00 (Morimoto et al., 1975a). Among these, 5*C* (Fe_9S_{10}), 11*C* ($Fe_{10}S_{11}$), and 6*C* ($Fe_{11}S_{12}$) are more abundant than phases with non-integer values of *N* and are therefore regarded as comparatively more stable (Morimoto et al., 1975b). For simplicity, only 5*C* is indicated. Natural and synthetic monoclinic pyrrhotite (4*C*) is believed by most authors to have a composition of Fe_7S_8 at low temperatures (Kissin and Scott, 1982); however, a solid-solution range of up to 0.02 in x units has been reported by some workers (calculated from data compiled by Kullerud, 1986).

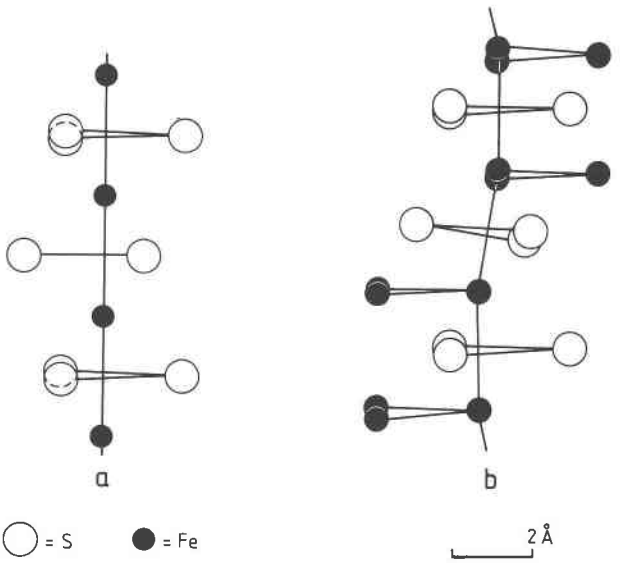

Fig. 2. (**a**) Configuration of S and Fe atoms along **c** (vertical in fig.) in the NiAs structure. (**b**) Configuration in the troilite structure, which contains triangular clusters of three Fe atoms. Each Fe atom is surrounded by a distorted sulfur octahedron. The troilite cell can be derived from the NiAs cell by doubling the **c** axis, with the **a** axes deviating by 30° in a plane $\perp$ **c**.

Experimental methods

Fe powder of 99.999% purity (Johnson Matthey) was inserted in a silica tube and heated at ~970 K for two hours in a stream of H_2 gas to reduce oxide traces in the material. Depending on the desired sample composition, appropriate amounts of reduced Fe and S (Ventron, 99.9999% purity) were weighed. The charge, typically 200 mg, was then inserted into a glass tube into which a piece of quartz wool was pushed with a glass rod. The tube was evacuated and sealed with the quartz wool and rod remaining, thus reducing the free volume to a minimum. The tube was subsequently heated at 823 K for a few days and then cooled to room temperature. The products were homogenized by grinding under acetone for one hour, and the loading procedure was repeated. Samples were annealed at 773 K to 963 K (see Table 1) for at least 30 h followed by quenching in ice water. Samples in the compositional range $0.004 \leq x \leq 0.143$ were apparently homogeneous. However, one sample with composition $x \approx 0.155$ was poorly crystallized and showed phase segregation immediately after quenching. A Mössbauer spectrum showed probable pyrite peaks.

Experimental products were mixed with KCl and analyzed by X-ray diffractometry using Cu radiation at room temperature. Peaks were located with $2\theta = 0.01°/s$ scans in the interval $5° \leq 2\theta \leq 85°$ and recorded at 0.001°/s. A scan made immediately after a measurement indicated that no oxidation had affected the sample.

The pyrrhotite 102 peak was checked to ensure that only the hexagonal structure was present (Kissin, 1974). Corrections of d-values were made with second-degree polynomials calculated for each diffraction pattern using six KCl peaks. Values of x were obtained from d_{102} according to an empirical equation of Yund and Hall (1969), which gives a standard error of ± 0.002 in x. NiAs subcell parameters were computed from eight pyrrhotite peaks.

Transmission Mössbauer data were obtained using a ^{57}CoRh source with a constant acceleration drive. Powdered absorbers containing ~5 mg Fe/cm^2 were spread

on a horizontal Be disk and inserted into a vacuum chamber that was kept at 285 ± 2 K using tap water as a cooling medium. For measurements at 77 K, samples were placed between pieces of adhesive tape and inserted into a LN_2 cryostat. Velocity scale calibrations were made with an iron foil at room temperature. X-ray diffraction patterns obtained for three samples before and after measurement of Mössbauer data showed a maximum difference in x of 0.002 and no phase segregation.

The original 512-channel Mössbauer spectra, containing an average of $1.1 \cdot 10^7$ pulses per channel, were folded and then fitted by a full Hamiltonian program (Jernberg and Sundqvist, 1983). The quadrupole splitting was defined as $QS = 0.5 V_{zz} eQ(1 + (\eta^2)/3)^{0.5}$, following the method of van Dongen Torman et al. (1975). Absorbers were thin and hence lines were assumed to be Lorentzian; consequently, no thickness corrections were made.

Table 1. Selected crystallographic data for syntheses

x	d_{102} (Å)	a (Å)	c (Å)	T_a (K)
0.0043	2.0925	3.4464(3)	5.8717(6)	773
0.0104	2.0910	3.4466(3)	5.8620(6)	773
0.0187	2.0890	3.4474(5)	5.8496(9)	773
0.0241	2.0876	3.4476(4)	5.8443(6)	773
0.0258	2.0872	3.4477(3)	5.8396(5)	773
0.0365	2.0845	3.4488(4)	5.8256(8)	773
0.0416	2.0832	3.4491(6)	5.8189(11)	773
0.0509*	2.0807	3.4555(4)	5.7920(7)	773
0.0517*	2.0805	3.4556(4)	5.7911(6)	773
0.0544	2.0798	3.4554(6)	5.7911(10)	773
0.0555	2.0795	3.4556(5)	5.7873(8)	773
0.0574	2.0790	3.4551(3)	5.7834(5)	773
0.0789	2.0729	3.4507(4)	5.7556(7)	773
0.1061	2.0647	3.4437(2)	5.7225(4)	623
0.1106	2.0632	3.4427(4)	5.7153(7)	673
0.1111**	2.0631	3.4425(3)	5.7151(5)	773
0.1203†	2.0601	3.4380(6)	5.7024(10)	893
0.1271†	2.0578	3.4372(2)	5.6971(3)	883
0.1324	2.0560	3.4364(3)	5.6903(5)	773
0.1367	2.0545	3.4345(3)	5.6831(5)	803
0.1384	2.0539	3.4339(3)	5.6814(4)	823
0.1431	2.0522	3.4331(3)	5.6758(5)	873
~0.155‡	2.048	3.411(4)	5.709(8)	963

Note: Chemical compositions are computed from d_{102} and are given by x in $Fe_{1-x}S$. Cell parameters are given for the NiAs subcell. Annealing temperature is indicated by T_a.

* Segregation after a few days, Mössbauer spectrum excluded.

** No Mössbauer data.

† Contained magnetite, spectrum excluded.

‡ Phase segregation immediately after quenching.

Results and discussion

Diffractometry

The values of c and a obtained for the NiAs subcell are given in Figures 3 and 4, respectively. Linear relationships are shown by c vs. x along two separate trends, and by a vs. x for small x values. The discontinuities in plots of a and c at $x \approx 0.045$ amount to 0.2% in both cases.

The data of Barker and Parks (1986) clearly show a discontinuity in c vs. x similar to the present one; however, this was not noted by the authors.

Phase transition

The relations between cell parameters and x in synthetic $Fe_{1-x}S$ have been investigated by several authors. Fleet (1968) obtained sharp discontinuities in parameters at $x \approx 0.047$, similar to those in Figures 3 and 4. For $x \leq 0.047$, Fleet observed a $\sqrt{3}A/2C$ supercell, consistent with the troilite structure (Hägg and Sucksdorff, 1933). For the samples with $x \leq 0.042$ of the present study, the troilite structure was indicated by the superstructure reflections described by Fleet. Bertaut (1956) and Evans (1970) described this structure (hexagonal, space group $P\bar{6}2c$), which includes triangular clusters of three Fe atoms in a plane $\perp$ **c**. Pairs of clusters are stacked above one another along **c**, with alternating pairs situated obliquely above or below. Thus, a line connecting Fe atoms along **c** is alternately parallel and inclined to **c** (Fig. 2b). According to Goodenough (1962), the clusters are caused by Fe-Fe bonds formed by 3d electrons when Fe-Fe distances decrease below a critical value. The troilite structure, and hence the clusters, cease to exist at the α transition. When the temperature is increased to $T_\alpha \approx$ 413 K, FeS transforms from troilite to an MnP-type structure (King and Prewitt, 1982). With an increase in pressure T_α decreases (Kullerud et al., 1965) and is equal to room temperature at a pressure of 3.4 GPa for FeS (King and Prewitt, 1982). Sparks et al. (1962) obtained neutron-diffraction data for synthetic $Fe_{1-x}S$, $x \approx 0$. They observed discontinuous changes in lattice parameters as temperature decreased through T_α, c increasing ~1% and a decreasing ~0.5%.

The discontinuities in plots of a vs. x and c vs. x observed in this study might be explained as follows. The decrease in c associated with an increase of x in the interval $0 \leq x \leq 0.042$, or an increase in pressure (King and Prewitt, 1982) for $x = 0$, is equivalent to decreasing Fe-Fe distances along **c**. The average distances from a given Fe atom to its four nearest Fe neighbors in the troilite structure are given in Figure 5 as a function of x. As x increases, the distance to the atoms obliquely above or below becomes even smaller than that within the cluster. It is therefore possible that the d bonding in the cluster is disturbed and eventually disrupted; i.e., an α transition occurs. The increase in distance between the atoms formerly constituting the cluster would then cause a sudden increase in **a** and decrease in **c**. The changes in a and c observed in the present study are not as large as those of Sparks et al. (1962); however, the α transition becomes less accentuated with increasing x, with a decreasing **c**-axis contraction (Moldenhauer and Brückner, 1976).

Samples with $x = 0.051$ and 0.052 were apparently homogeneous immediately after quenching but showed broadening and splitting of the 102 peak after measurement of Mössbauer data at 283 K for 3 and 7 d, respectively, indicating phase segregation. Thus, a determination of x_α at room temperature must take kinetic effects into consideration.

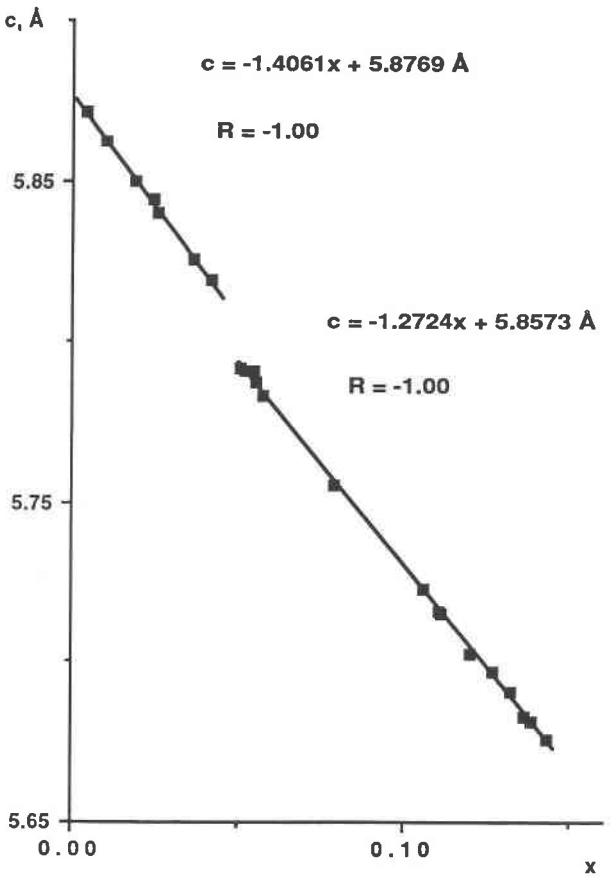

Fig. 3. Magnitude of c for the NiAs subcell vs. x. The largest standard deviation in a value of c is ±0.001, i.e., within squares. Equations derived by least-squares and correlation coefficients R are given.

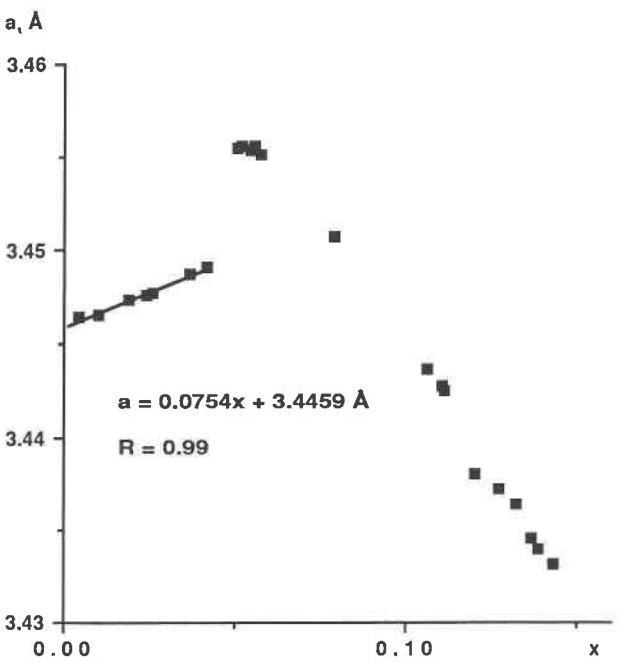

Fig. 4. Magnitude of a for the NiAs subcell vs. x. The largest standard deviation in a value of a is ±0.0006, i.e., within squares. Equation derived by least-squares and R are given for the linear region of the plot.

Mössbauer spectroscopy

The spectra obtained can be divided into three categories, depending on the composition of the samples: (1) $0.004 \leq x \leq 0.042$, (2) $0.054 \leq x \leq 0.079$, and (3) $0.106 \leq x \leq 0.143$; see Figure 6 for typical spectra. The interval 1, within which the troilite structure has been reported, shows one strong sextet and additional sextets of low intensity. Interval 2 is characterized by broad peaks and interval 3 by three well-resolved sextets, or possibly six. Data at 77 K were obtained for samples with $x = 0.079$ and $x = 0.143$. On visual inspection, the broadening of the spectrum of the sample with $x = 0.079$ appeared to be due to the superposition of at least seven subspectra. Each of the three well-resolved sextets for $x = 0.143$ was shown to consist of at least two subspectra.

Interval $0.004 \leq x \leq 0.042$. A total of three sextets have been assumed: A (largest intensity I and hyperfine field B_{hf}), B (intermediate I and B_{hf}), and C (smallest I and B_{hf}). The line widths w of all sextets in a spectrum were constrained to be equal. In the fitting routine, variations in the asymmetry parameter η of the electric field gradient tensor ($\eta = (V_{xx} - V_{yy})/V_{zz}$) have been shown to have only very minor influence on the angle θ between $\mathbf{B}_{hf}$ and the largest component of the field tensor, $\mathbf{V}_{zz}$, in meteoritic troilite (Kruse and Ericsson, 1988); therefore, η was set to zero. In addition, ϕ (the angle between the projection of $\mathbf{B}_{hf}$ on the $\mathbf{V}_{xx} - \mathbf{V}_{yy}$ plane and $\mathbf{V}_{xx}$) was set to zero, since it is undefined if $\eta = 0$. In subspectrum B, θ showed strong dependence on the intensity of C. In the final fittings, θ for B was therefore fixed at 35°, which is the arithmetic mean for fittings of three spectra where θ was variable and the influence of C was weak. No convergence of θ values could be determined for C and hence θ was set equal to zero for these subspectra.

Parameters for $x \leq 0.042$ are given in Table 2. Possible solutions for sextet A ($x = 0.004$) were $QS = 1.1$ and $\theta = 61°$, or $QS = -0.86$ and $\theta = 48°$. The latter fit yielded a somewhat smaller χ^2 value; in addition, Hafner and Kalvius (1966) and Kruse and Ericsson (1988) determined that negative QS solutions were more likely for natural troilites; thus, parameters are given here with negative QS values. Since $\mathbf{B}$ of the Fe atoms is $\parallel \mathbf{c}$ for the present compositions and temperatures (Horwood et al., 1976), a value of $\theta = 48°$ would agree with $\mathbf{V}_{zz}$ being oriented along the shortest Fe-S distance (~2.33 Å, at an angle of ~50° to c).

Parameters for A conform well with those obtained by Kruse and Ericsson (1988). It can thus be assumed that A represents Fe atoms without adjacent vacancies, similar to the situation in troilite. By qualitative comparison, C would correspond to a very different environment and

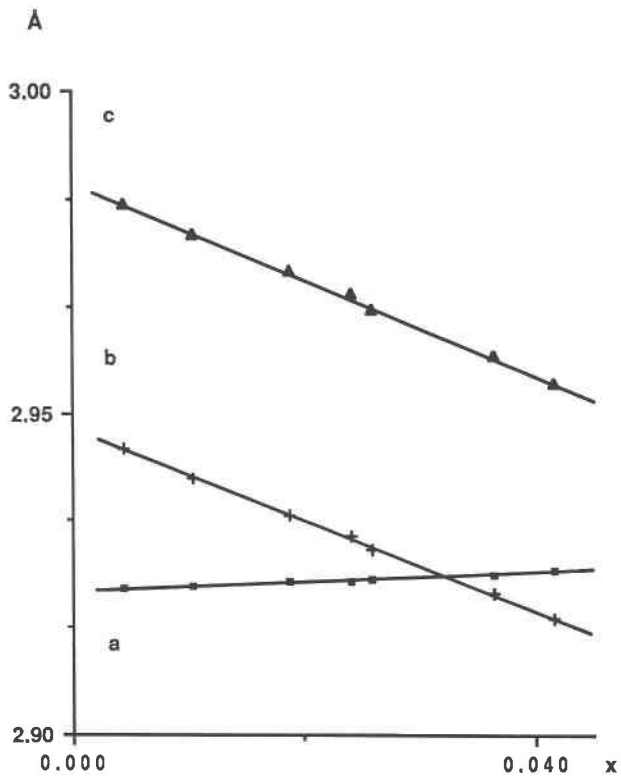

Fig. 5. Average Fe-Fe distances in the troilite structure vs. x. (**a**) within a cluster, (**b**) between neighbors obliquely above or below (see Fig. 2b), and (**c**) between neighbors directly above or below. Points are derived from observed data and fitted with straight lines. In addition, four more near Fe-atom neighbors occur at distances 3.7 and 3.8 Å in the same plane $\perp$ **c**.

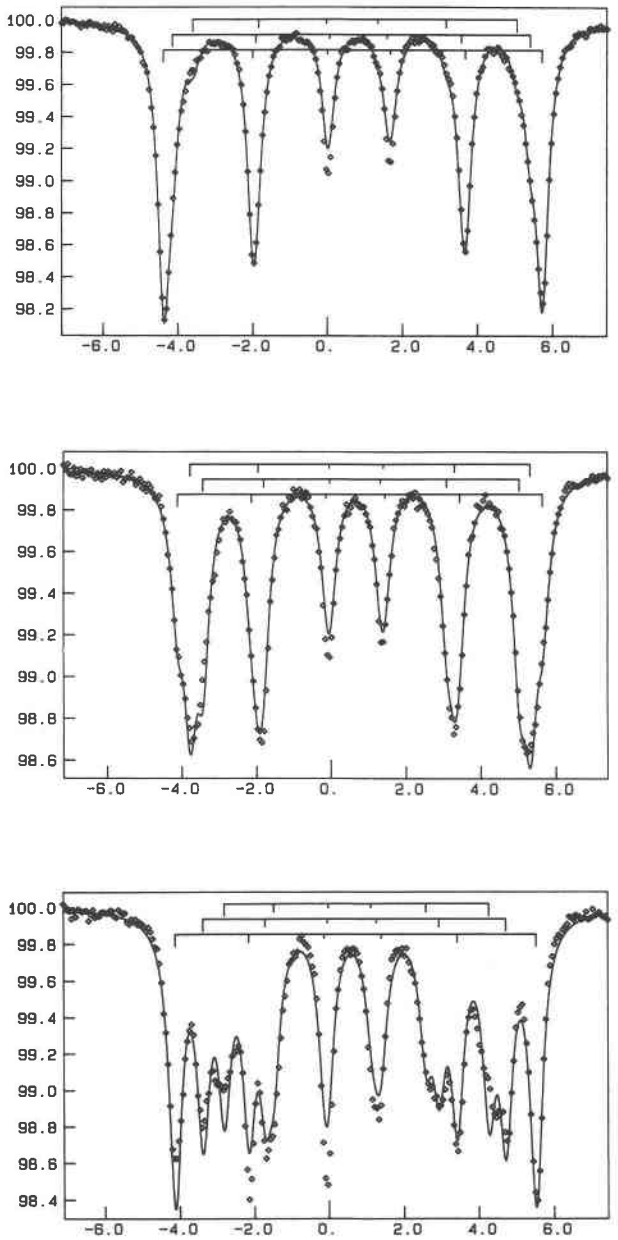

Fig. 6. Mössbauer spectra of $Fe_{1-x}S$. **Top**: $x = 0.037$ at 283 K, **middle**: $x = 0.079$ at 286 K, and **bottom**: $x = 0.143$ at 283 K. Transmission in percent vs. γ source velocity in mm/s. Sextets are indicated by bar diagrams. The strong sextet in the top spectrum is absent in the lower two.

B to an intermediate case. An Fe atom in troilite has eight nearest Fe neighbors at a distance ≤ 3.8 Å. Six surround it in the same plane, two of which are members of the same cluster, plus one above and one below. A vacancy would cause a very different environment for two Fe atoms, since these would not be members of any cluster. The fraction of Fe atoms with such an environment is $F_1 = 100 \cdot 2x/(1 - x)$ percent for any sample. The vacancy would, to a lesser extent, also affect the nearby Fe atoms that are cluster members. Assuming the influence to be important within the 3.8 Å distance, six Fe atoms would be affected. If the concentration of vacancies is low, the fraction of such Fe atoms is $F_2 = 100 \cdot 6x/(1 - x)$. Hence, the fraction of relatively unaffected Fe atoms is $F_3 = 100 - (F_1 + F_2)$, and thus F_3 corresponds to A, F_2 to B, and F_1 to C. Obtained I values and computed fractions are given in Figure 7. The similarities in their trends and magnitudes indicate that the above assignment may be justified.

The small variation of hyperfine parameters with varying x indicates that the Fe positions are affected only to a very minor degree by the vacancy concentration. If the above assignment is accepted, a comparison between unaffected Fe atoms (A) with those that are not cluster members (C) gives B_{hf} and centroid shift (CS) values 4.2 T and 0.05 mm/s larger for A. These differences are the same as between coexisting troilite and FeS with the MnP-type structure (Kruse and Ericsson, 1988) and might reflect the difference in state for an Fe atom being a cluster member or not, rather than the presence of a nearby vacancy. The charge of Fe in troilite is +0.66 in electron units (Marusak and Tongson, 1979), indicating consid-

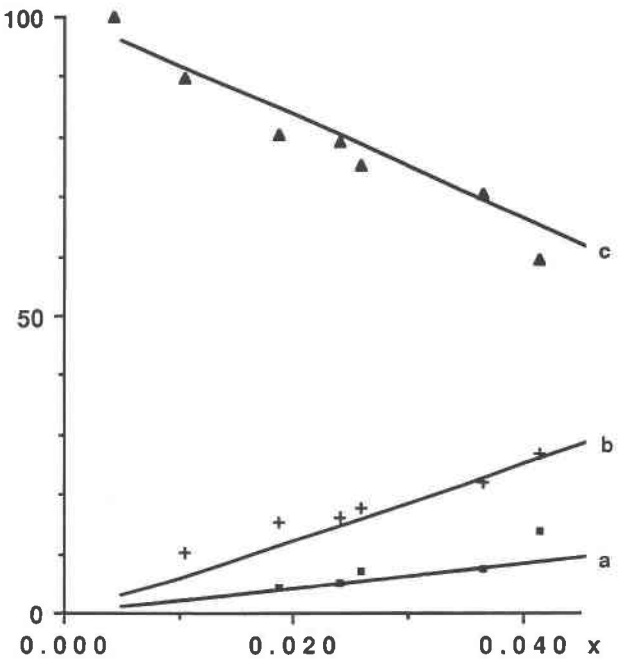

Fig. 7. The measured intensities of sextets and computed concentrations of Fe atoms within different environments, in percent vs. x within the range $0.004 \leq x \leq 0.042$. (a) Squares: intensities of the sextet with smallest B_{hf}; line: $F_1 = 100 \cdot 2x/(1 - x)$; (b) crosses: intensities of the intermediate B_{hf} sextet; line: $F_2 = 100 \cdot 6x/(1 - x)$; (c) triangles: intensities of the sextet with the largest B_{hf}; line: $F_3 = 100 - (F_1 + F_2)$.

Table 2. Mössbauer parameters for samples with $0.004 \leq x \leq 0.042$

x	Sextet	I %	w (mm/s)	CS (mm/s)	B_{hf} (T)	QS (mm/s)	θ (°)
0.004	A	100	0.31	0.76	31.1	−0.86	48
0.010	A	90	0.35	0.76	31.1	−0.85	47
	B	10	0.35	0.73	29.7	−0.39	35!
0.019	A	80	0.36	0.76	31.1	−0.82	47
	B	15	0.36	0.74	29.8	−0.39	35!
	C	4	0.36	0.70	26.9	0.04	0!
0.026	A	75	0.35	0.76	31.0	−0.83	46
	B	18	0.35	0.74	29.5	−0.39	35!
	C	7	0.35	0.70	26.8	0.06	0!
0.042	A	60	0.37	0.76	31.0	−0.79	46
	B	27	0.37	0.74	29.3	−0.34	35!
	C	14	0.37	0.72	26.9	0.07	0!

Note: Data for a total of seven samples were measured; those excluded had values of both x and Mössbauer parameters close to the listed ones. Owing to low intensities of sextets B and C, spectra for samples with $x = 0.004$ and 0.010 were fitted with one and two sextets, respectively. The sign "!" indicates that the parameter was set to the listed value in the fitting.

erable covalency. According to Goodenough (1978), one paired 3d electron per Fe atom is delocalized upon cluster formation. Since the Fe is in the high-spin state, the remaining five 3d electrons are all unpaired and of parallel spin and thus may induce an increase in B_{hf} at the nucleus. The four parallel spins of a C-type Fe correspond to a B_{hf} of 26.9 T, or 6.7 T per electron. An A-type Fe with five parallel spins would thus give a value of B_{hf} of $5 \cdot 6.7 = 33.6$ T. If the delocalized electron retains its spin and spends some of its time adjacent to the Fe atom, then the resulting effect on B_{hf} would be less. Thus, the value of 31.1 T determined for A-type Fe might be explained. The smaller decrease in B_{hf} and CS for B as compared to A might be an effect of the loss of a near neighbor. The decrease in $|QS|$ from A to C is probably due to the increased site distortion.

Intervals $0.054 \leq x \leq 0.079$ and $0.106 \leq x \leq 0.143$. Intervals 2 and 3 are not separated by any cell-parameter discontinuity. Hence, it is likely that the crystal structures are similar. Despite the differences in appearance of spectra, it can therefore be assumed that the intervals may be treated together in the discussion of Mössbauer data. Because of the good peak separation in interval 3, an analysis should start there.

The structures of the samples of this study are derivatives of the NiAs structure. Rows of Fe atoms alternating with staggered S-triangles occur along the c-axis. Every Fe atom is therefore surrounded by six S atoms, the S triangles forming planes $\perp$ c, which is a threefold rotation axis. Since only Fe positions may be vacant, these symmetry relations remain essentially intact with nearby vacancies. Therefore, η and ϕ were set to zero for all sextets in the fittings. The w values were constrained to be equal for the subspectra. Fitting of the vague (283 K) and clearly visible (77 K) six subspectra for $x = 0.143$ was not successful and hence a simplified three-sextet model was applied for interval 3: D for the largest value of B_{hf}, E for the intermediate value and F for the smallest value. Resultant parameters are given in Table 3.

For each sextet in interval 3, two equally possible sets of solutions were obtained for positive and negative values of QS. No further indication of the sign was indicated for data obtained at 77 K.

Bertaut (1953) proposed a model for the structure of natural pyrrhotite of composition Fe_7S_8, assuming repulsion between vacancies. Vacancy avoidance in $Fe_{1-x}S$ has also been discussed by Powell (1983). Tokonami et al. (1972) confirmed and refined the structure, which contains three structural environments for the Fe atoms: zero, one, or two vacancies among the eight nearest Fe positions. Mössbauer spectra of natural (e.g., Hafner and Kalvius, 1966) and synthetic (e.g., Igaki et al., 1981) pyrrhotite, close to this composition, have accordingly been interpreted to consist of three sextets. The B_{hf} values given by Hafner and Kalvius (1966) were 30.7, 25.5, and 22.5 T; those of the present sextets are 30.1, 25.5, and 22.7 T for the same composition ($x = 0.12$, interpolated values). It can therefore be assumed that these environments are present in interval 3. Since no visible sextets in addition to the mentioned ones occur, the cases of three or more vacancies among the nearest neighbors may be excluded from the discussion.

At high temperatures, the vacancy distribution is ran-

TABLE 3. Mössbauer parameters for samples with $0.106 \leq x \leq 0.143$

x	Sextet	I %	w (mm/s)	CS (mm/s)	B_{hf} (T)	QS (mm/s)	θ (°)
0.106	D	41	0.35	0.70	30.1	−0.54/0.30	64/41
	E	37	0.35	0.69	26.1	−0.54/0.31	60/47
	F	21	0.35	0.68	23.4	−0.48/0.31	75/31
0.111	D	42	0.36	0.69	30.2	−0.48/0.27	64/41
	E	36	0.36	0.68	25.7	−0.59/0.35	60/46
	F	23	0.36	0.67	23.1	−0.45/0.31	75/32
0.132	D	42	0.33	0.68	30.0	−0.33/0.19	66/39
	E	33	0.33	0.66	25.3	−0.51/0.36	59/49
	F	25	0.33	0.67	22.2	−0.53/0.36	74/32
0.143	D	43	0.38	0.68	29.9	−0.24/0.15	67/38
	E	31	0.38	0.66	25.0	−0.41/0.36	61/49
	F	26	0.38	0.66	21.9	−0.42/0.32	76/33

Note: Data for a total of six samples were measured; those excluded had values of both x and Mössbauer parameters close to the listed ones. Two sets of equally possible solutions were obtained for each sextet: one for negative and one for positive values of QS; corresponding θ values are given in the same order.

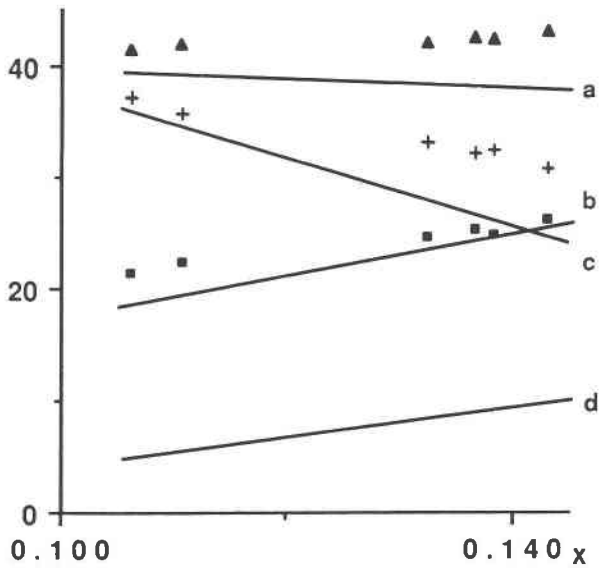

Fig. 8. The measured intensities I of sextets in the interval $0.106 \leq x \leq 0.143$ and computed probabilities of Fe atoms within different environments, in percent vs. x. (a) probability of one vacancy among the eight nearest Fe positions ($P(1v/8)$), (b) $P(2v/8)$, (c) $P(0v/8)$, (d) the forbidden case $P(3v/8)$. $P(4v/8)$ is less than 2.5% throughout the measured interval. Triangles: I of the sextet with the largest value of B_{hf}; crosses: I of the intermediate B_{hf} sextet; squares: I of the sextet with smallest B_{hf}.

dom (Morimoto, 1978). Since diffusion-dependent reactions are extremely slow below 573 K (Kissin and Scott, 1982), this distribution is assumed to be maintained during quenching and measurement of data, with the limitation that only zero, one, or two vacancies are allowed among the nearest neighbors. The probability of any Fe position being vacant is x. The vacancy probability of an occupied Fe position may be regarded as being divided among the surrounding eight Fe positions. Thus, the probability of any one of these positions being vacant will be $x' = 9/8 \cdot x$. The probability P of an Fe atom having a given number n of vacancies v among the eight neighboring positions was therefore computed as $P(nv/8) = [(1 - x')^{8-n} \cdot x'^{n} 8!]/(8 - n)! \cdot n!$ where $0 \leq n \leq 8$. Since there is no algorithm for the exclusion of forbidden cases from the computations, the magnitude of P for the allowed cases is only approximate. Obtained I values for interval 3 and probabilities for $0 \leq n \leq 3$ are given in Figure 8. An assignment, based on a comparison of intensities and probabilities, indicates that D, E, and F are associated with the 1v/8, 0v/8, and 2v/8 positions, respectively.

B_{hf} of sextet D is approximately constant at about 30 T, whereas those of E and F increase with decreasing x. D reflects a decrease in $|QS|$ with increasing x, whereas no definite trend can be established for F. For the present temperatures and compositions, the magnetic moments of the Fe atoms are aligned $\perp$ **c** (Horwood et al., 1976). If the spins are assumed to be aligned along the shortest Fe-Fe separations in the plane (i.e., $\parallel$ **a**) and E represents a 0v/8 position, then the θ value of ~48° for the positive QS solutions for this sextet would correspond to $\mathbf{V}_{zz}$ being oriented along the shortest Fe-S separation in the NiAs structure (2.45 Å and an angle of 45° with **a** for $x = 0.106$).

A comparison of the spectra indicates that D and E are also present in interval 2. No F sextets were observed, which indicates that the 2v/8 positions are absent. The fitting in interval 2 was made with the assumption that D and E are still present and that they represent equally well-defined positions. The remaining subspectra, appearing principally as peaks between those of D and E, were all fitted as sextet G. The value of w for D and E was therefore fixed at the value 0.35 mm/s, which is the average for the sextets in the well-resolved spectra of interval 3. The influence of the subspectra in G could not be resolved, and hence w for G was free to vary. Results are given in Table 4.

B_{hf} values for D and E conform well with those of interval 3, thus supporting the above assumption. The intermediate values of G might represent Fe atoms with 0v/8 and 1v/8 affected by vacancies beyond the eight nearest Fe positions. The next-nearest neighboring positions consist of 12 sites, six in each of the planes above and below. The environment of an Fe atom with 0v/8 could be modified by a vacancy in either of the planes, or in both planes. Depending on the position of the nearest vacancy at a site with 1v/8, one or two additional vacancies are allowed. The modified environments would cause a decrease in B_{hf} of an Fe atom with 1v/8 and increase that of an Fe atom with 0v/8, in a manner that is similar to the cases 1v/8 → 2v/8 and 0v/8 → 1v/8 in interval 3. The increase in the concentration of vacancies and modified sites is reflected by an increase in I and w of G. The general and continuous decrease of CS with increasing x for intervals 2 and 3 conforms with the decrease in cell volume. As in interval 3, QS for E is inferred to be positive.

TABLE 4. Mössbauer parameters for samples with $0.054 \leq x \leq 0.079$

x	Sextet	I %	w (mm/s)	CS (mm/s)	B_{hf} (T)	QS (mm/s)	θ (°)
0.054	D	29	0.35!	0.78	30.3	−0.88/0.87	54/56
	E	30	0.35!	0.75	26.7	−0.39/0.22	74/30
	G	41	0.36	0.75	28.7	−0.41/0.19	73/22
0.056	D	24	0.35!	0.77	30.1	−0.84/0.89	55/53
	E	31	0.35!	0.75	26.6	−0.41/0.26	71/33
	G	45	0.39	0.75	28.6	−0.38/0.18	75/18
0.057	D	22	0.35!	0.77	30.1	−0.91/0.95	55/53
	E	30	0.35!	0.75	26.5	−0.38/0.27	72/34
	G	48	0.42	0.75	28.5	−0.42/0.15	72/14
0.079	D	16	0.35!	0.72	29.8	−1.00/0.95	58/52
	E	30	0.35!	0.73	26.3	−0.34/0.27	73/33
	G	54	0.50	0.72	28.4	−0.35/0.13	68/11

Note: Owing to difficulties in resolving subspectra, w of sextets D and E was fixed and that of G (representing several subspectra) was free to vary. Depending on the sign of QS, two sets of possible solutions were obtained for each sextet. Based on the appearance of fitted functions in comparison to data points, QS and θ combinations giving superior solutions are underlined.

Vaughan et al. (1971) obtained Mössbauer data for natural pyrrhotite. Hexagonal samples showed broad peaks and poorly resolved sextets, as in interval 2, whereas monoclinic pyrrhotite showed relatively well-separated sextets, as in interval 3. For equilibrated syntheses, the maximum x value for hexagonal pyrrhotite has been given as, e.g., 0.097 (dry synthesis, Yund and Hall, 1969), and 0.105 (hydrothermal synthesis, Kissin and Scott, 1982). The defined boundaries occurring towards higher x values in the T vs. x phase diagrams are very steep, which indicates that composition and not temperature is most important in determining which structure is formed. Monoclinic pyrrhotite is reported for larger x values, e.g., in the interval $0.115 \leq x \leq 0.134$ (hydrothermal synthesis, Kissin and Scott, 1982). The intervals 2 and 3 largely coincide with those where hexagonal and monoclinic pyrrhotite, respectively, may be synthesized. Since Fe atoms with 2v/8 for the temperatures of the present study might only be allowed in interval 3, it is possible that the occurrence of this environment is a necessary (although not the only) requirement for the formation of stable monoclinic pyrrhotite. With increased temperature, the repulsive electrostatic forces forbidding 2v/8 environments may be overcome. If vacancies are simultaneously ordered into every other Fe layer stacked along c, then monoclinic pyrrhotite of $4C$ type might form. The monoclinic structure may be regarded as the result of a slight distortion of the hexagonal structure (Flahaut, 1972), in which the c axis tilts with respect to the basal plane; the tilt angle β for monoclinic Fe_7S_8 is 90.6° (Corlett, 1968). A structural transformation related to the vacancy reordering mentioned above would explain the negative slopes of the hexagonal pyrrhotite–hexagonal pyrrhotite + $4C$ monoclinic pyrrhotite boundaries in the phase diagram (Fig. 1) and the occurrence of Λ-type ferrimagnetism (named after the Λ-shaped magnetization vs. temperature curve) attributed to the $4C$ superstructure in the interval 450–540 K for $x = 0.092$ (Marusak and Mulay, 1979).

The B_{hf} vs. x trend for C and E is continuous. If E represents Fe with 0v/8 in intervals 2 and 3, then this trend would support the assumption that C reflects the state of an Fe atom not being a cluster member rather than being one with a near-neighbor vacancy.

ACKNOWLEDGMENTS

Thanks are due to Hans Annersten, Tore Ericsson, and Örjan Amcoff for critically reviewing the manuscript. I would also like to thank F.K. Madis Roots for many fruitful discussions.

REFERENCES CITED

Barker, W.W., and Parks, T.C. (1986) The thermodynamic properties of pyrrhotite and pyrite. A re-evaluation. Geochimica et Cosmochimica Acta, 50, 2185–2194.

Bertaut, E.F. (1953) Contribution a l'étude des structures lacunaires: la pyrrhotine. Acta Crystallographica, 6, 557–561 (in French).

——— (1956) Structure de FeS stoechiométrique. Bulletin de la Société française de Minéralogie et de Cristallographie, LXXIX, 276–292.

Corlett, M. (1968) Low-iron polymorphs in the pyrrhotite group. Zeitschrift für Kristallographie, 126, 124–134.

Evans, H.T. (1970) Lunar troilite: Crystallography. Science, 167, 621–623.

Flahaut, J. (1972) Transition metal chalcogenides. In L.E.J. Roberts, Ed., MTP International Review of Science, Solid State Chemistry, Inorganic Chemistry Series One, vol. 10, p. 189–240. Butterworths University Park Press, London.

Fleet, M.E. (1968) On the lattice parameters and superstructures of pyrrhotites. American Mineralogist, 53, 1846–1855.

Goncharov, G.N., Ostanevich, Yu.M., Tomilov, S.B., and Cser, L. (1970) Mössbauer effect in the FeS_{1+x} system. Physica Status Solidi, 37, 141–150.

Goodenough, J.B. (1962) Cation-cation three-membered ring formation. Journal of Applied Physics, supplement to 33:3, 1197–1199.

——— (1978) Structural chemistry of iron sulfides. Materials Research Bulletin, 13, 1305–1314.

Gosselin, J.R., Townsend, M.G., Tremblay, R.J., and Webster, A.H. (1976) Mössbauer effect in single-crystal $Fe_{1-x}S$. Journal of Solid State Chemistry, 17, 43–48.

Hafner, S., and Kalvius, M. (1966) The Mössbauer resonance of Fe^{57} in troilite (FeS) and pyrrhotite ($Fe_{0.88}S$). Zeitschrift für Kristallographie, 123, 443–458.

Hägg, G., and Sucksdorff, I. (1933) Die Kristallstruktur von Troilit und Magnetkies. Zeitschrift für Physikalische Chemie B, 22, 444–452.

Horwood, J.L., Townsend, M.G., and Webster, A.H. (1976) Magnetic susceptibility of single-crystal $Fe_{1-x}S$. Journal of Solid State Chemistry, 17, 35–42.

Igaki, K., Sato, M., and Shinohara, T. (1981) Mössbauer study on the iron vacancy distribution in iron sulfide $Fe_{1-x}S$ ($0.083 \leq x \leq 0.125$). Transactions of the Japan Institute of Metals, 22, 627–632.

——— (1982) Mössbauer study on the distribution of iron vacancies in iron sulfide $Fe_{1-x}S$. Transactions of the Japan Institute of Metals, 23, 221–228.

Jernberg, P., and Sundqvist, T. (1983) A versatile Mössbauer analysis program. Uppsala University Institute of Physics Reports 1090.

King, H.E., and Prewitt, C.T. (1982) High-pressure and high-temperature polymorphism of iron sulfide (FeS). Acta Crystallographica B, 38, 1877–1887.

Kissin, S.A. (1974) Phase relations in a portion of the Fe-S system. Ph.D. thesis, University of Toronto, Canada (not seen; extracted from Mineralogical Society of America Short Course Notes: Sulfide Mineralogy, S-22 and CS-25, 1974).

Kissin, S.A., and Scott, S.D. (1982) Phase relations involving pyrrhotite below 350 °C. Economic Geology, 77, 1739–1754.

Kruse, O., and Ericsson, T. (1988) A Mössbauer investigation of natural

troilite from the Agpalilik meteorite. Physics and Chemistry of Minerals, 15, 509–513.

Kullerud, G., Bell, P.M., and England, J.L. (1965) High pressure differential thermal analysis. Carnegie Institution Annual Report of the Director, Geophysical Laboratory, 1964–1965, 197–199.

Kullerud, G. (1986) Monoclinic pyrrhotite. Bulletin of The Geological Society of Finland, 58, 293–305.

Marusak, L.A., and Mulay, L.N. (1979) Mössbauer and magnetic study of the antiferro to ferrimagnetic phase transition in Fe_9S_{10} and the magnetokinetics of the diffusion of iron during the transition. Journal of Applied Physics, 50, 1865–1867.

Marusak, L.A., and Tongson, L.L. (1979) Soft X-ray emission and Auger electron spectroscopic study of FeS, $Fe_{0.9}S$, $Fe_{0.875}S$, and $Fe_{0.5}S$. Journal of Applied Physics, 50, 4350–4355.

Moldenhauer, W., and Brückner, W. (1976) Physical properties of nonstoichiometric iron sulfide $Fe_{1-x}S$ near the α-phase transition. Physica Status Solidi (a), 34, 565–571.

Morimoto, N., Gyobu, A., Tsukuma, K., and Koto, K. (1975a) Superstructure and nonstoichiometry of intermediate pyrrhotite. American Mineralogist, 60, 240–248.

Morimoto, N., Gyobu, A., Mukaiyama, H., and Izawa, E. (1975b) Crystallography and stability of pyrrhotites. Economic Geology, 70, 824–833.

Morimoto, N. (1978) Direct observation of the superstructures of nonstoichiometric compounds by high resolution electron microscopy. Memoirs of the Institute of Scientific and Industrial Research, Osaka University, 36, 45–59.

Nakazawa, H., and Morimoto, N. (1971) Phase relations and superstructures of pyrrhotite, $Fe_{1-x}S$. Materials Research Bulletin, 6, 345–358.

Ono, K., Ito, A., and Hirahara, E. (1962) Mössbauer study of hyperfine field, quadrupole interaction, and isomer shift of Fe^{57} in $FeS_{1.00}$, $FeS_{1.05}$ and $FeS_{1.07}$. Journal of the Physical Society of Japan, 17, 1615–1620.

Onufrienok, V.V., and Zvegintsev, A.G. (1982) Magnetic properties and crystal structure of iron sulfides in the composition range of FeS-$FeS_{1.18}$. Inorganic Materials, 18, 301–304 (translated from Izvestiya Akademii Nauk SSSR, Neorganicheskie Materialy, vol. 18, no. 3, 366–368, 1982).

Ovanesyan, N.S., Trukhtanov, V.A., Odinets, G.Yu., and Novikov, G.V. (1971) Vacancy distribution and magnetic ordering in iron sulfides. Soviet Physics Journal of Experimental and Theoretical Physics, 33, 1193–1197 (translated from Zhurnal Eksperimental'noi i Teoreticheskoi Fiziki, 60, 2220–2229, 1971).

Powell, R. (1983) Thermodynamic mixing properties of pyrrhotine, $Fe_{1-x}S$. Mineralogical Magazine, 47, 437–440.

Putnis, A., and McConnell, J.D.C. (1980) Principles of mineral behaviour, 257 p. Blackwell Scientific Publications, Oxford/Elsevier, New York.

Schwartz, E.J., and Vaughan, D.J. (1972) Magnetic phase relations of pyrrhotite. Journal of Geomagnetism and Geoelectricity, 24, 441–458.

Sparks, J.T., Mead, W., and Komoto, T. (1962) Neutron diffraction investigation of the magnetic and structural properties of near-stoichiometric iron sulfide. Journal of the Physical Society of Japan, 17B-I, 249–251.

Tokonami, M., Nishiguchi, K., and Morimoto, N. (1972) Crystal structure of a monoclinic pyrrhotite (Fe_7S_8). American Mineralogist, 57, 1066–1080.

van Dongen Torman, J., Jagannathan, R., and Trooster, J.M. (1975) Analysis of ^{57}Fe Mössbauer hyperfine spectra. Hyperfine Interactions, 1, 135–144.

Vaughan, D.J., Schwarz, E.J., and Owens, D.R. (1971) Pyrrhotites from the Strathcona mine, Sudbury, Canada: A thermomagnetic and mineralogical study. Economic Geology, 66, 1131–1144.

Yund, R.A., and Hall, H.T. (1969) Hexagonal and monoclinic pyrrhotites. Economic Geology, 64, 420–423.

Manuscript received August 9, 1989
Manuscript accepted April 10, 1990